White phosphorescent organic light-emitting diodes using double emissive layer with three dopants for color stability

Jin Wook Kim[1], Nam Ho Kim[1], Ju-AnYoon[1], Seung Il Yoo[1], Jin Sung Kang[1], and Woo Young Kim[1,2*]

[1]*Department of Green Energy & Semiconductor Engineering, Hoseo University, Asan, South Korea*

[2]*Department of Engineering Physics, McMaster University, Hamilton, ON L8S 4L7, Canada*

[*]*Corresponding author: wykim@hoseo.edu*

Received May 19, 2014; accepted July 16, 2014; posted online September 26, 2014

We fabricate white phosphorescent organic light-emitting diodes (PHOLEDs) with three dopants and double emissive layer (EML) to achieve color stability. The white PHOLEDs use FIrpic dopant for blue EML (B-EML), and $Ir(ppy)_3$:$Ir(piq)_3$ dopants for green:red EML (GR-EML) with *N*,*N*′-dicarbazolyl-3, 5-benzene (mCP) as host material. Thicknesses of B-EML and GR-EML are adjusted to form a narrow recombination zone at two EML's interface and charge trapping happens in EML according to wide highest occupied molecular orbital and/or lowest unoccupied molecular orbital energy band gap of mCP and smaller energy band gap of dopants. The total thickness of both EMLs is fixed at 30 nm in the device structure of ITO (150 nm)/MoO_3 (2 nm)/*N*,*N*′-diphenyl-*N*,*N*′-bis(l-naphthyl-phenyl)-(l,l′-biphenyl)-4, 4′-diamine (70 nm)/mCP:Firpic-8.0% (12 nm)/mCP:$Ir(ppy)_3$-3.0%:$Ir(piq)_3$-1.5% (18 nm)/2′,2′,2″-(1,3,5-benzinetriyl)-tris(1-phenyl-1-H-benzimidazole) (30 nm)/8-hydroxyquinolinolato-lithium (2 nm)/Al (120 nm). White PHOLED shows 18.25 cd/A of luminous efficiency and white color coordinates of (0.358 and 0.378) at 5000 cd/m^2 and color stability with slight CIE_{XY} change of (0.028 and 0.002) as increasing luminance from 1000 to 5000 cd/m^2.

OCIS codes: 300.2140, 300.6170, 330.1690, 230.3670.

doi: 10.3788/COL201412.102302.

Organic light-emitting diodes (OLEDs) have heralded a new section in chemistry and physics since a stack of organic thin films were demonstrated to be an efficient light-emitting structure in 1987[1]. Especially, phosphorescent OLEDs (PHOLEDs) with white emission spectra are promising candidates for future lighting source because of their potential applications in solid-state lighting to realize extremely high quantum efficiency compared with conventional fluorescent OLEDs (FLOLEDs) which utilizes both singlet and triplet excitons for light emission[2–7]. For color stable white emission, it is essential to control a combination of three primary colors (blue, green, and red) or at least two contemporary colors using different dopants via concentration and/or position adjustment in emissive layer (EML), considering exciton's intrinsic property which normally moves from higher triplet state to lower triplet state[8–15]. When primary color dopants (blue, green, and red) are close to each other within Dexter energy transfer radius, respectively, energy transfer certainly acts such as exciton's nature characteristics previously mentioned. Therefore, usually red dopant which has lower triplet state can be saturated first and then green and blue consecutively. As a result, color shift from red to green or blue as increasing the current density is inevitable. It is well-known that highest occupied molecular orbital (HOMO) and/or lowest unoccupied molecular orbital (LUMO) of dopants, when compared with host materials can trap holes and/or electrons[16–18]. Charge trapping can lead to direct recombination of holes and electrons on dopants[19,20].

Here we fabricated white PHOLEDs with double EML such as ITO (150 nm)/MoO_3 (2 nm)/*N*,*N*′-diphenyl-*N*,*N*′-bis(l-naphthyl-phenyl)-(l,l′-biphenyl)-4,4′-diamine (NPB) (70 nm)/*N*,*N*′-dicarbazolyl-3 5-benzene (mCP): Firpic-8.0%(x nm)/mCP:$Ir(ppy)_3$-3.0%:$Ir(piq)_3$-z% (y nm)/2′,2′,2″-(1,3,5-benzinetriyl)-tris(1-phenyl-1-H-benzimidazole) (TPBi) (30 nm)/8-hydroxyquinolinolato-lithium (Liq) (2 nm)/Al (120 nm) using FIrpic as blue dopant and $Ir(ppy)_3$ and $Ir(piq)_3$ as green and red dopants. To achieve color stability of white emission, narrow recombination zone was formed at two EMLs' interface via adjusting thicknesses of both blue EML (B-EML) x nm and green:red EML (GR-EML) y nm simultaneously to demonstrate deep charge trapping of green and red dopant molecules and then the concentration z% of $Ir(piq)_3$ which has lower triplet state limiting saturation under the total thickness of EML fixed at 30 nm. Figure 1 shows the energy band diagrams and triplet energy levels of white PHOLED device.

To fabricate OLED devices, ITO-coated glass substrates with a sheet resistance of ~12 Ω/sq were used. Line patterns of ITO were formed on glass by photolithography process. The ITO glass was cleaned in an ultrasonic bath by the regular cleaning sequences: in deionized water, isopropyl alcohol, acetone, deionize water, and isopropyl alcohol, thereafter, the pre-cleaned ITO glass was treated with O_2 plasma under vacuum

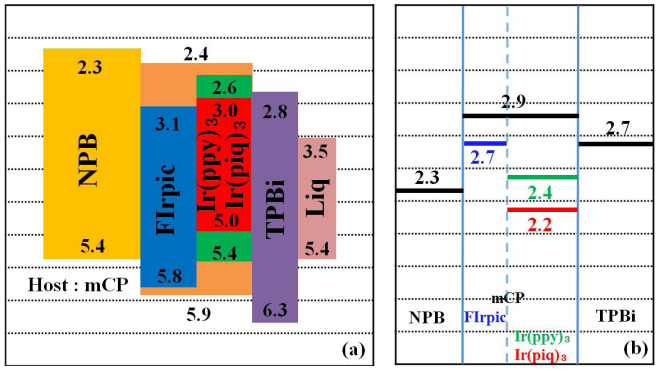

Fig. 1. (a) Energy band diagrams and (b) triplet energy levels of the white PHOLED device.

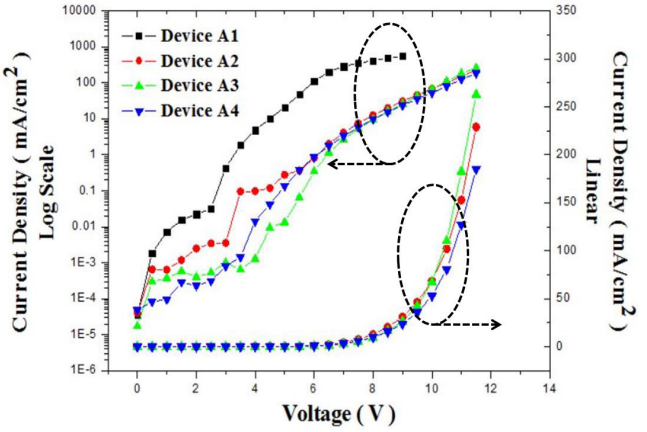

Fig. 2. Current density–voltage characteristics of PHOLED devices A1, A2, A3, and A4 with log and regular y-axis scale.

conditions of 5.0×10^{-2} Torr, of 50 W for 2 min, and then MoO_3 as hole injection layer was deposited by thermal evaporation. All organic materials were deposited by thermal evaporation technique under a pressure of ~1.0×10^{-7} Torr. White PHOLEDs composed of NPB as a hole transporting layer (HTL) material, mCP as host material, Bis(3,5-difluoro-2-(2-pyridyl)-phenyl-(2-carboxypyridyl)iridium III (Firpic) as blue doped into mCP in B-EML, tris(2-phenylpyridine) iridium(III) ($Ir(ppy)_3$), and tris(1-phenylisoquinoline) iridium(III) ($Ir(piq)_3$) as green and red doped into mCP in GR-EML, respectively, TPBi as electron transfer layer, and Liq as electron injection layer, respectively. Then aluminum cathode electrode was deposited by thermal evaporation with evaporation rate of 0.5 nm/s. The electro–optical characteristics of the white PHOLED devices were measured and analyzed using a Keithley 238 LMS PR-650 spectrophotometer, colorimeter, and the IVL system.

In order to demonstrate the proof of deep charge trapping on FIrpic, $Ir(ppy)_3$, and $Ir(piq)_3$ molecules as blue, green, and red dopants in mCP as host which has wide band gap (E_g = 3.5 eV) in EML, we fabricated devices A1, A2, A3, and A4 in order such as ITO (150 nm)/MoO_3 (2 nm)/NPB (70 nm)/EML (30 nm)/TPBi (30 nm)/Liq (2 nm)/Al (120 nm), where EML = mCP:-non-doping, mCP:FIrpic-8.0%, mCP:$Ir(ppy)_3$-3.0%, and mCP:$Ir(piq)_3$-1.0%, respectively, to demonstrating phenomenon of charge trapping. As shown in Fig. 1, the difference in HOMO energy levels between mCP and $Ir(piq)_3$ is 0.9 eV, and the difference in LUMO energy levels between mCP and $Ir(ppy)_3$ is 0.5 eV, whereas the difference between mCP and FIrpicis is 0.1 eV. It can be expected that devices A3 and A4 have a more possibility of deep hole trapping than device A2 because HOMO energy levels of $Ir(piq)_3$ and $Ir(ppy)_3$ are higher (closer to vacuum level) than that of FIrpic and mCP as described in Fig. 1. Figure 2 shows two plots of current density–voltage (J–V) of the devices A1, A2, A3, and A4 with different y-axis scale to clearly confirm their tendency at lower and higher current densities. As shown in Fig. 2, there is unstable current density curve of the devices A2, A3, and A4 in lower voltage region that may suggest existence of leakage currents. However, the current density curve of the devices A2, A3, and A4 shows charge carrier's trapping effect clearly even though there is a possibility of leakage current. There appeared different shapes of J–V curves between higher and lower driving voltage on the basis of 4 V. The rapid increase in the current density of the devices A2, A3, and A4 after 4 V can be explained by space-charge-limited current due to saturated trapping center, whereas J–V curve's characteristics at lower voltage before 4 V is affected by charge trapping. Current density of device A1 is superior to devices A2, A3, and A4 because of non-doping EML without charge-trapping system by dopant molecules causing an increase in driving voltage of the PHOLEDs. The amount of initial current density in the single EML devices is in order of A1, A2, A3, and A4 at 1–3 V of driving voltage. However, current density curve of the device A4 intersected that of device A3 at 3.5 V and did again at 8.5 V as driving voltage increased. And also current density curve of the device A3 intersected that of device A2 at 10.5 V as driving voltage increased. These results can be explained as follows: there are two main factors for the reversal of current density curve between three devices such as direct hole trapping system by FIrpic, $Ir(ppy)_3$, and $Ir(piq)_3$ molecules and NPB's mobility as HTL much faster than TPBi's electron mobility as electron transporting layer, which suggests NPB has an influence in the amount of current density at EML. As shown in Fig. 1, HOMO energy levels of NPB and $Ir(ppy)_3$ are 5.4 eV each, and holes injected from anode to NPB can move into the $Ir(ppy)_3$ molecules first in EML without the interruption because there is no energy barrier between HOMO levels of NPB and $Ir(ppy)_3$. However, initial current density curve of device A3 is lower than that of device A2 and it can certainly prove that there are no injected holes until saturation of hole trapping by $Ir(ppy)_3$ molecules. After saturation of hole trapping by $Ir(ppy)_3$ molecules, holes can contribute to current density causing an increase in the driving voltage of device A3 which has

0.5 V higher HOMO energy level than the device A1. On the other hand, initial current density curve of device A4 is lower than that of device A3 but intersected soon at 3.5 V due to lower doping concentration of $Ir(piq)_3$ which can be saturated quickly.

We fabricated PHOLED devices B1–B4 with double EML structure using FIrpic for B-EML and $Ir(ppy)_3$ for G-EML without $Ir(piq)_3$ for R-EML under ITO (150 nm)/MoO_3 (2 nm)/NPB (70 nm)/mCP:FIrpic-8.0% (x nm)/mCP:$Ir(ppy)_3$-3.0% (y nm)/TPBi (30 nm)/Liq (2 nm)/Al (120 nm), where x = 80, 100, 120, and 200 and also y = 220, 200, 180, and 100 to find out the recombination zone at the interface between double EMLs and observe electroluminescence (EL) spectra's behaviors by using charge-trapping system which is shown in Fig. 2. Figure 3 shows EL spectra of the devices B1, B2, B3, and B4 as luminance increased from 1000 to 10,000 cd/m^2. Peak intensity of the devices B1, B2, and B3 at 470 nm is reasonably similar to one another but it is slightly increased in the device B4 when luminance is changed to 10000 cd/m^2. Namely, peak intensity at 503 nm in the device B4 is decreased as the total luminance increased due to left shift of recombination zone from interface between B-EML and G-EML. On the other hand, the intensity of $Ir(ppy)_3$ in the devices B1 and B2 increased due to right shift of recombination zone from interface between two different EMLs considering their peak intensities at 470 nm but they are a little lower when the total luminance is changed from 1000 to 10000 cd/m^2. However, there is no peak intensity change of EL spectra in the device B3, which means it has good color stability as the luminance increased due to settled recombination zone at interface between two different EMLs by hole trapping on $Ir(ppy)_3$ molecules.

Figure 4 shows EL spectra of the devices C1–C4 as varying concentration of $Ir(piq)_3$ as red dopant from 0.5% to 2.0% under structure ITO (150 nm)/MoO_3 (2 nm)/NPB (70 nm)/mCP:FIrpic-8.0% (12 nm)/mCP:$Ir(ppy)_3$-3.0%:$Ir(piq)_3$-z% (12 nm)/TPBi (30 nm)/Liq (2 nm)/Al (120 nm) and it indicates that the intensity of red peak at 612 nm is proportional to concentration of $Ir(piq)_3$ under luminance of 1000 cd/m^2 but decreased as luminance increased to 5000 cd/m^2. These results can be explained as the $Ir(piq)_3$ molecules are saturated and then

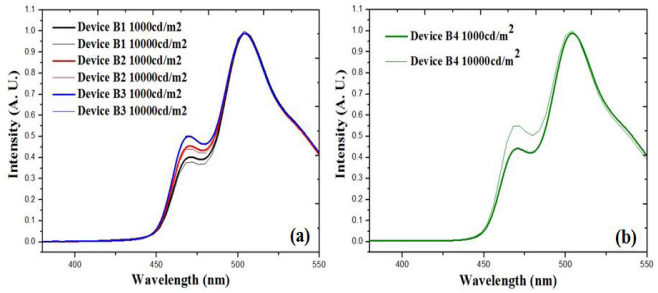

Fig. 3. EL spectra of PHOLED devices (a) B1, B2, and B3 and (b) B4 at different luminances.

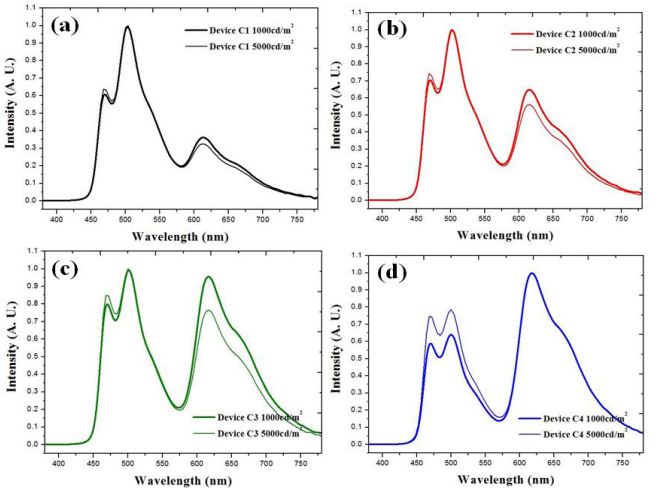

Fig. 4. EL spectra of white PHOLED device with varying concentration of $Ir(piq)_3$ (a) 0.5%, (b) 1.0%, (c) 1.5%, and (d) 2.0% as red dopant in EML at the luminance of 1000 and 5000 cd/m^2.

triplet excitons move back to FIrpic attributing more blue light emission. However, EL spectra of the device C4 are shown in Fig. 4(d). Figure 4(d) shows that peak intensities of FIrpic and $Ir(ppy)_3$ are lower at 1000 cd/m^2 compared with the other devices C1, C2, and C3, and then increased at 5000 cd/m^2 because triplet excitons contribute to more red light emission as concentration of $Ir(piq)_3$ increased at 2.0%. We should especially consider Dexter energy transfer between $Ir(ppy)_3$ with higher triplet state, and $Ir(piq)_3$ with lower triplet state in GR-EML because these dopant molecules are close to each other within Dexter energy transfer radius even though recombination zone is formed at interface between two different EMLs.

As shown in Table 1, there is no significant change in CIE_Y but a little shift of CIE_X due to Dexter energy transfer from FIrpic to $Ir(piq)_3$ according to the recombination happened at the interface between B-EML and GR-EML. Exciton scan transfer from $Ir(piq)_3$ to $Ir(ppy)_3$ molecules when $Ir(piq)_3$ molecules are getting saturated but FIrpic as blue dopant is more contributed to white emission when $Ir(piq)_3$ molecules are saturated

Table 1. Efficiency and Color Coordinates of White PHOLED Devices

Device	Efficiency[a] (cd/A)	Color Coordinates	
		ΔCIE_{XY}[b]	CIE_{XY}[a]
C1	31.24	(–0.011, –0.001)	(0.280, 0.429)
C2	22.57	(–0.019, –0.002)	(0.327, 0.401)
C3	18.25	(–0.028, –0.002)	(0.386, 0.380)
C4	13.35	(–0.033, 0.000)	(0.435, 0.353)

[a]Efficiency and CIE_{XY} at 1000 cd/m^2.

[b]CIE_{XY} difference at 1000 and 5000 cd/m^2.

if there is not much higher concentration of $Ir(piq)_3$ affected by excitons of $Ir(ppy)_3$ such as device C4. Therefore, EL peak intensity of $Ir(piq)_3$ as red dopant decreased whereas that of FIrpic increased, even though FIrpic and $Ir(piq)_3$ dopants existed in different EMLs, which can be explained that the recombination zone is located obviously at the interface between B-EML and GR-EML and possible energy transfer between FIrpic and $Ir(piq)_3$. Considering appropriate white light emission with color stability, device C3 shows reasonable CIE_{XY} color coordinates of (0.358 and 0.378) at 5000 cd/m^2 which are closer to ideal white CIE_{XY} color coordinates of (0.33 and 0.33) than the devices C1, C2, and C3 and 22.57 cd/A of luminous efficiency at 1000 cd/m^2.

In conclusion, we report the color stable structure of white PHOLEDs with double EML using concept of deep charge carrier trapping by dopant molecules. Deep hole and electron trapping mechanism in EML with narrow energy gaps of HOMOs and LUMOs between host and dopants are applied for confirming recombination zone in three dopants–double EML systems. We investigate color shift from red to green or blue as increasing the luminance from 1000 to 5000 cd/m^2 via formation of recombination zone at interface between B-EML and GR-EML by hole trapping on $Ir(ppy)_3$ molecules as green dopant and then the electron trapping on FIrpic molecules as blue dopant. Excited molecules of phosphorescent dopant $Ir(ppy)_3$ are formed by the sequential trapping of holes and electrons onto the organo–metallic complex. White PHOLED device C2 with structure of ITO (150 nm)/MoO_3 (2 nm)/NPB (70 nm)/mCP:Firpic-8.0% (12 nm)/mCP:$Ir(ppy)_3$-3.0%:$Ir(piq)_3$-1.5% (18 nm)/TPBi (30 nm)/Liq (2 nm)/Al (120 nm) shows the best electrical and optical performance as 18.25 cd/A of luminous efficiency at 1000 cd/m^2 and white color coordinates of (0.358 and 0.378) at 5000 cd/m^2 with ignorable change of (−0.028 and −0.002) changing luminance from 1000 to 5000 cd/m^2.

References

1. C. W. Tang and S. A. Van Slyke, Appl. Phys. Lett. **51,** 913 (1987).
2. M. A. Baldo, D. F. O'Brien, Y. You, A. Shoustikov, S. Sibley, M. E. Thompson, and S. R. Forrest, Nature **395,** 151 (1998).
3. G. He, M. Pfeiffer, K. Leo, M. Hofmann, J. Birnstock, R. Pudzich, and J. Salbeck, Appl. Phys. Lett. **85,** 3911 (2004).
4. M. A. Baldo, M. E. Thompson, and S. R. Forrest, Nature **403,** 750 (2000).
5. J. A. Yoon, Y. H. Kim, N. H. Kim, C. G. Jhun, S. E. Lee, Y. K. Kim, F. R. Zhu, and W. Y. Kim, Chin. Opt. Lett. **12,** 012032 (2014).
6. S. Huang, Z. Ye, J. Lu, Y. Su, C. Chen, and G. He, Chin. Opt. Lett. **11,** 062302 (2013).
7. L. Tang, H. Xia, P. Wang, J. Peng, and H. Jiang, Chin. Opt. Lett. **11,** 061603 (2013).
8. Y. H. Kim, K. W. Cheah, and W. Y. Kim, Appl. Phys. Lett. **103,** 053307 (2013).
9. Y. Sun, N. C. Giebink, H. Kanno, B. Ma, M. E. Thompson, and S. R. Forrest, Nature **440,** 908 (2006).
10. C. H. Hsiao, Y. H. Lan, P. Y. Lee, T. L. Chiu, and J. H. Lee, Org. Electron. **12,** 547 (2011).
11. L. C. Meng, Y. B. Hou, Z. D. Lou, F. Teng, X. Yao, X. J. Liu, A. W. Tang, and J. B. Peng, Synth. Met. **172,** 63 (2013).
12. C. H. Hsiao, S. W. Liu, C. T. Chen, and J. H. Lee, J. Appl. Phys. **106,** 024503 (2009) .
13. W. S. Jeon, T. J. Park, S. Y. Kim, R. Pode, J. Jang, and J. H. Kwon, Org. Electron. **10,** 240 (2009).
14. L. Hou, L. Duan, J. Qiao, D. Zhang, G. Dong, L. Wang, and Y. Qui, Org. Electron. **11,** 1344 (2010).
15. Y. S. Tsai, L. A. Hong, F. S. Juang, and C. Y. Chen, J. Lumin. **153,** 312 (2014).
16. T. C. Liao, H. T. Chou, F. S. Juang, Y. S. Tsai, S. H. Wang, V. Tuan, and Y. Chi, Curr. Appl. Phys. **11,** 175 (2011).
17. Y. Zhao, L. Zhu, J. Chen, and D. Ma, Org. Electron. **13,** 1340 (2012).
18. C. B. Moon, W. Song, M. Meng, N. H. Kim, J. A. Yoon, W. Y. Kim, R. Wood, and P. Mascher, J. Lumin. **146,** 314 (2014).
19. F. Nuesch, D. Berner, E. Tutis, M. Schaer, C. Ma, X. Wang, B. Zhang, and L. Zuppiroli, Adv. Funct. Mater. **15,** 323 (2005).
20. H. Fukagawa, T. Shimizu, Y. Osada, T. Kamada, Y. Kiribayashi, T. Yamamoto, and N. Shimidzu, Appl. Phys. Express **6,** 052104 (2013).